Syntheses, Characterizations, and X-ray Structures of Alkali Metal Derivatives of Titanium(IV) Neopentoxides

Timothy J. Boyle,* Todd M. Alam, Cory J. Tafoya, and Eric R. Mechenbier

Advanced Materials Laboratory, Sandia National Laboratories, 1001 University Boulevard, S.E., Albuquerque, New Mexico 87106

Joseph W. Ziller

Department of Chemistry, University of California—Irvine, Irvine, California 92717

Received September 24, 1998

Reactions of titanium(IV) neopentoxide, [Ti(μ-O*neo*-Pe)(O*neo*-Pe)$_3$]$_2$ (**1**, O*neo*-Pe = OCH_2CMe_3), with alkali neopentoxides (AO*neo*-Pe) resulted in the isolation of the dimeric complexes [ATi(O*neo*-Pe)$_5$]$_2$ [A = Li (**2**), Na (**3**), and K (**4**)], independent of the alkali metal investigated. Each compound was characterized by solution and solid-state multinuclear NMR, isopiestic molecular weight determination, and/or single-crystal X-ray diffraction. In the solid state, both **2** and **4** were found to adopt a standard [MM′(OR)$_5$]$_2$ arrangement, wherein the Ti metals are in a distorted trigonal-bipyramidal geometry and each alkali metal center is four-coordinated. Suitable crystals of **3** were not isolated, but solid-state MAS (^{17}O, ^{13}C, ^{x}A) NMR spectroscopy indicated that the solid-state structure of **3** was consistent with its congeners. Multinuclear (^{1}H, ^{7}Li, ^{13}C, ^{17}O, ^{23}Na) solution NMR spectroscopy data in toluene revealed that **2** exists in a complex multinuclear equilibrium, whereas **3** and **4** exist as mononuclear species in solution.

Introduction

Metal alkoxides (M(OR)$_x$) have been extensively investigated as precursors for high-quality ceramic thin films.[1−4] These precursors are widely used due to their high solubility and stability in a variety of solvents, relatively low decomposition/crystallization temperatures, and commercial availability. While stoichiometric mixtures of M(OR)$_x$ have been found to be an excellent method for the preparation of complex ceramic thin films, "single-source" precursors are also of continued interest. A viable pathway for generating these single-source starting materials is to derivatize the parent alkoxide with an alkali metal (eq 1) followed by a metathesis reaction with the desired metal halide (eq 2).[5]

$$\mathrm{M(OR)}_x + \mathrm{AOR} \rightarrow \text{“AM(OR)}_{x+1}\text{”} \quad (1)$$

$$y\text{“AM(OR)}_{x+1}\text{”} + \mathrm{M'Cl}_y \xrightarrow{-y\mathrm{ACl}} \text{“M'[M(OR)}_{x+1}]_y\text{”} \quad (2)$$

A commonly used precursor for titanium containing materials is Ti(OPr^i)$_4$ (OPr^i = $OCHMe_2$). This precursor has been modified with alkali metal *iso*-propoxide (AOPr^i, where A = Li, Na, K) and was found to form compounds of the general formula "ATi(OPr^i)$_5$" (eq 3). However, upon metathesis the "Ti(OPr^i)$_5^-$" moiety does not always cleanly transfer. In an

$$\mathrm{Ti(OPr^i)_4} + \mathrm{AOPr^i} \rightarrow [\mathrm{ATi(OPr^i)_5}]_n \quad (3)$$
$$\mathrm{A = Li},\ n = 2;\ \mathrm{Na},\ n = \infty;\ \mathrm{K},\ n = \infty$$

effort to understand this phenomenon, we reported the solution and structural aspects of the "ATi(OPr^i)$_5$" series.[5] For this family of compounds only the lithium derivative was isolated as a molecular species. [LiTi(OPr^i)$_5$]$_2$ was crystallographically characterized in a standard M_4O_{16}-like arrangement wherein the titanium and lithium atoms were found to adopt a distorted trigonal-bipyramidal (tbp) and tetrahedral geometry, respectively. The Na and K congeners of the "ATi(OPr^i)$_5$" compounds were isolated as linear and nonlinear polymeric chains, respectively. Parts A−C of Figure 1 are thermal ellipsoid plots of [LiTi(OPr^i)$_5$]$_2$, [NaTi(OPr^i)$_5$]$_\infty$, and [KTi(OPr^i)$_5$]$_\infty$, respectively. It was also noted in this report that for the "ATi(OPr^i)$_5$" and ASn(OBu^t)$_3$ systems, A/M cation ratios greater than 1.4 yielded polymeric structures in the solid state.

For M(OR)$_x$ complexes, the size, shape, and type of the pendant hydrocarbon chain of the alkoxide groups plays a determining role in the final structure.[1−4] We have been investigating the neopentoxide (O*neo*-Pe = OCH_2CMe_3) ligand for the development of new precursors for the production of thin films of metal oxide ceramics.[6−9] The O*neo*-Pe ligand is attractive for thin film applications for two reasons: (i) the

* To whom correspondence should be addressed.

(1) Bradley, D. C.; Mehrotra, R. C.; Gaur, D. P. *Metal Alkoxides*; Academic Press: New York, 1978.
(2) Bradley, D. C. *Chem. Rev.* **1989**, *89*, 1317.
(3) Chandler, C. D.; Roger, C.; Hampden-Smith, M. J. *Chem. Rev.* **1993**, *93*, 1205.
(4) Hubert-Pfalzgraf, L. G. *New. J. Chem.* **1987**, *11*, 663.
(5) Boyle, T. J.; Bradley, D. C.; Hampden-Smith, M. J.; Patel, A.; Ziller, J. W. *Inorg. Chem.* **1995**, *34*, 5893.
(6) Boyle, T. J.; Alam, T. M.; Mechenbeir, E. R.; Scott, B.; Ziller, J. W. *Inorg. Chem.* **1997**, *36*, 3293.
(7) Boyle, T. J.; Alam, T. A.; Dimos, D.; Moore, G. J.; Buchheit, C. D.; Al-Shareef, H. N.; Mechenbier, E. R.; Bear, B. R. *Chem. Mater.* **1997**, *9*, 3187.
(8) Boyle, T. J.; Gallegos, J. J., III; Pedrotty, D. M.; Mechenbier, E. R.; Scott, B. L. *J. Coord. Chem.* **1999**, *155*.
(9) Boyle, T. J.; Pedrotty, D. M.; Scott, B.; Ziller, J. W. *Polyhedron* **1997**, *17*, 1959.

10.1021/ic981143d CCC: $18.00
Published on Web 04/22/1999

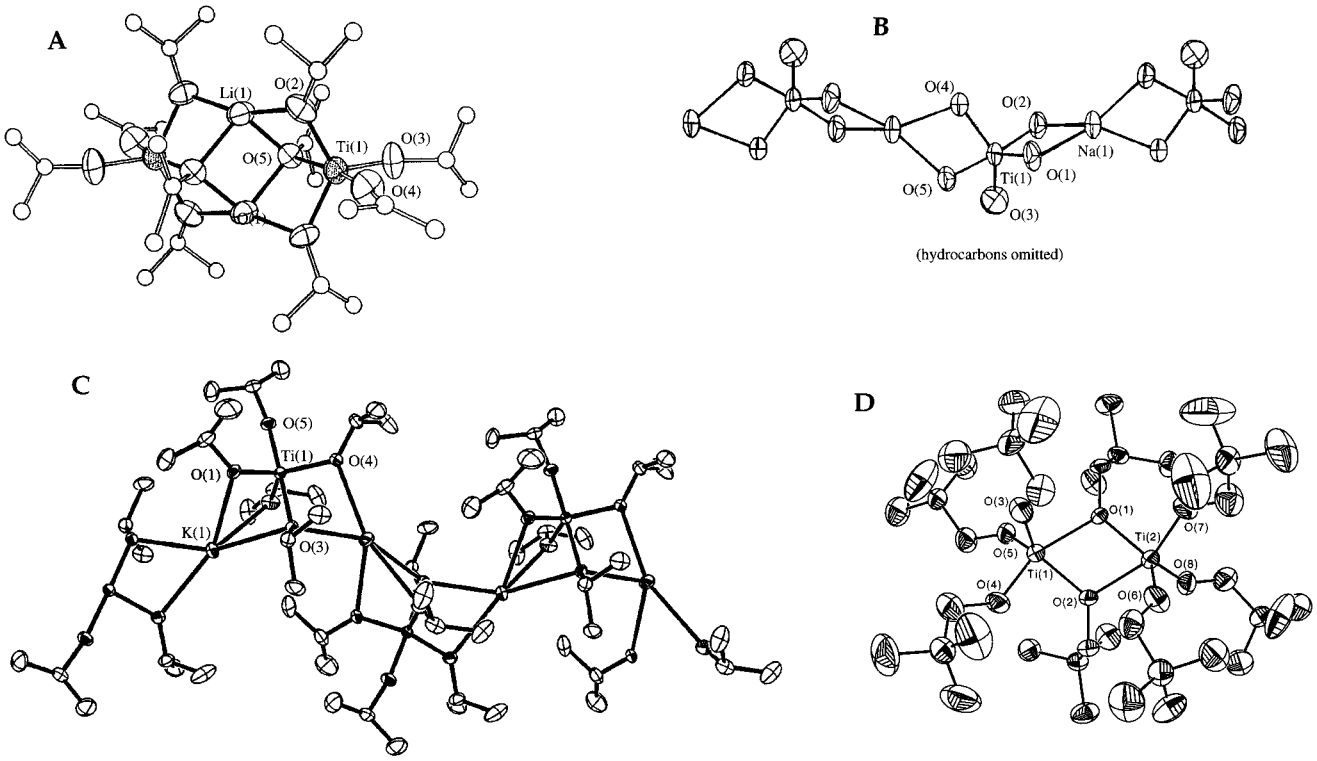

Figure 1. Thermal ellipsoid plots of: (A) $[LiTi(OPr^i)_5]_2$, (B) $[NaTi(OPr^i)_5]_\infty$, (C) $[KTi(OPr^i)_5]_\infty$ and (D) $[Ti(\mu\text{-}O\textit{neo}\text{-Pe})(O\textit{neo}\text{-Pe})_3]_2$, **1**.

β-hydrogens permit "cross-linking" of metal centers upon exposure to atmospheric humidity, yielding uniform films, and (ii) the *tert*-butyl moiety, due to steric hindrance, minimizes oligomerization and increases the solubility of the modified species. The reaction of $Ti(OPr^i)_4$ with excess HO*neo*-Pe resulted in the formation of $[Ti(\mu\text{-}O\textit{neo}\text{-Pe})(O\textit{neo}\text{-Pe})_3]_2$ (**1**, Figure 1D), the smallest crystallographically characterized homoleptic titanium alkoxide.[6] It was of interest to determine how the O*neo*-Pe ligands would effect the structure types adopted in comparison to the well-characterized OPr^i derivatives. Therefore, we report on the syntheses, solid-state structures, and solution behaviors of $[ATi(O\textit{neo}\text{-Pe})_5]_2$ (**2**, Li; **3**, Na; **4**, K) compounds. Where appropriate, a comparison between the O*neo*-Pe ligated species and the OPr^i derivatives is also presented.

Experimental Section

All reactions were performed under a dry argon atmosphere, using standard Schlenk, vacuum line, and glovebox techniques. Solvents were freshly distilled from, and stored over, the appropriate drying agents, as previously described.[7] All samples were of crystalline purity. Thermogravimetric analysis and differential thermal analysis (TGA/DTA) were obtained on an Omnitherm STA 1500 PL Thermal Sciences Analyzer using 8−15 mg of each compound loaded in air into a preweighed alumina boat and then heated under ultrahigh-pressure oxygen at a ramp rate of 5°/min from ambient temperature to 600 °C. FT-IR data were obtained on a Nicolet, Magna System Spectrometer-550 under an atmosphere of flowing N_2. Elemental analyses were performed on a Perkin-Elmer 2400 CHN-S/O elemental analyzer.

Solution NMR spectra were obtained on a DRX400 NMR spectrometer. ^1H and $^{13}C\{^1H\}$ NMR spectra were referenced against the residual proton or carbon resonances in toluene-d_8 at a resonant frequency of 400.1 and 100.6 MHz, respectively, using a 5 mm broadband probe. For the ^{13}C spectra a Waltz16 proton decoupling sequence was employed. DEPT 135 ^{13}C spectra were obtained using a standard pulse sequence, allowing the number of attached protons to be determined. For the $^{6,7}Li$ and ^{23}Na NMR investigations 1.0 M solutions of LiCl in D_2O and of NaCl in D_2O, respectively, were used as the standard external references.

Complex **1** was prepared according to the published reports.[7] AO*neo*-Pe was isolated from a reaction between the appropriate alkali metal or alkali metal hydride and (excess) HO*neo*-Pe (Aldrich) in toluene at reflux temperatures and purified by sublimation. Only the synthesis of **2** is detailed since similar syntheses were used for each of the following derivatives.

$[LiTi(OCH_2CMe_3)_5]_2$ (2). LiO*neo*-Pe (0.12 g, 2.39 mmol) in toluene (∼5 mL) was added to a predissolved solution of **1** (0.50 g, 0.63 mmol) in toluene (∼5 mL). This reaction mixture was stirred for 12 h, during which time a precipitate formed. The solution was then diluted to 30 mL and warmed slightly on a hot plate until the precipitate was completely dissolved. Upon cooling to glovebox temperatures, X-ray quality crystals (yield, 0.47 g (75.8%)) were isolated and proved to be $[LiTi(OCH_2CMe_3)_5]_2$, **2**. The removal of all of the volatile material from the reaction mixture yields a white powder. The crystalline and bulk powder had identical analytical data. ^1H NMR (400.1 MHz, toluene-d_8): δ 3.79(2H, s, OCH_2CMe_3), 3.61(3.6H, s, OCH_2CMe_3), 1.03 (9H, s, OCH_2CMe_3), 0.98 (17H, s, OCH_2CMe_3). $^{13}C\{^1H\}$ NMR (100.6 MHz, toluene-d_8): δ 77.5, 76.8 (OCH_2CMe_3), 34.3 (OCH_2CMe_3), 27.6, 26.9 (OCH_2CMe_3). FT-IR (KBr pellet, cm^{-1}): 2952 (m), 2885 (w), 1460 (w), 1452 (w), 1398 (w), 1342 (w), 1262 (w), 1103 (m), 1058 (mb), 1015 (m), 963 (w), 955 (w), 899 (w), 801 (w), 742 (w), 693 (w), 615 (w), 606 (w), 451 (w). TGA/DTA (oxygen) [weight loss up to °C (% total weight loss)/thermal event (°C)]: 200 °C (62%)/sm endo (55 °C), sm endo (170 °C), lg exo (193 °C); 300 °C (72%)/sm endo (205 °C), sm exo (240 °C), sm endo (285 °C); 500 °C (81%)/sm exo (335 °C).

$[NaTi(OCH_2CMe_3)_5]_2$ (3). Reaction stoichiometry: **1** (0.50 g, 0.63 mmol), NaO*neo*-Pe (0.14 g, 1.26 mmol) in toluene (∼15 mL), diluted to 25 mL. Crystalline yield: 0.37 g (57.8%). ^1H NMR (400.1 MHz, toluene-d_8): δ 4.00 (1H, s, OCH_2CMe_3), 0.98 (5.2H, s, OCH_2CMe_3). $^{13}C\{^1H\}$ NMR (100.6 MHz, toluene-d_8): δ 86.4 (OCH_2CMe_3), 34.1 (OCH_2CMe_3), 26.4 (OCH_2CMe_3). FT-IR (KBr pellet, cm^{-1}): 2950 (w), 2865 (m), 2700 (w), 1466 (w), 1478 (w), 1458 (m), 1392 (w), 1361 (w), 1258 (w), 1077 (s, br), 1023 (m), 932 (w), 900 (w), 797 (m), 751.19(w), 694 (m), 654 (w), 617 (w), 568 (w), 465 (m). TGA/DTA (oxygen) [weight loss up to °C (% total weight loss)/thermal event (°C)]: 105 °C (26%)/sm endo (48 °C); 285 °C (64%)/sm exo (240 °C); 500 °C, (70%)/lg endo (315 °C); 500 °C (22.7%).

$[KTi(OCH_2CMe_3)_5]_2$ (4). Reaction stoichiometry: **1** (0.20 g, 0.25 mmol), KO*neo*-Pe (0.06 g, 0.51 mmol) in toluene (~ 5 mL), diluted to 20 mL. Crystalline yield: 0.089 g (34.2%). ^{1}H (400.1 MHz, C_6D_6): δ 4.44 (1.0H, mult, μ_3-OCH_2CMe$_3$), 4.19 (1.5H, bs, *term*-OCH_2CMe$_3$), 4.04 (1.7H, s, μ-OCH_2CMe$_3$), 1.21 (1.6H, mult, OCH$_2$CMe_3), 1.05 (11.1H, s, OCH$_2$CMe_3), 0.98 (11.1H, s, OCH$_2$CMe_3). ^{13}C{^{1}H} NMR (100.6 MHz, C_6D_6) δ 87.0 (OCH_2CMe$_3$), 84.0 (OCH_2CMe$_3$), 34.8 (OCH$_2$$CMe_3$), 34.6 (OCH$_2$$CMe_3$), 27.9 (OCH$_2CMe_3$), 26.9 (OCH$_2CMe_3$). FT-IR (KBr pellet, cm^{-1}): 2950 (m), 2887 (m, br), 1491 (m), 1449 (m), 1390 (m), 1334 (m), 1240 (w), 1205 (w), 1115 (m, br), 1062 (s, br), 1009 (m), 925 (w), 907 (w), 763 (w), 707 (m), 689 (m), 631 (m), 596 (w), 493 (w), 479 (w). TGA/DTA (oxygen) [weight loss up to °C (% total weight loss)/thermal event (°C)]: 250 °C (61%) /lg exo (225 °C); 550 °C (67%)/lg exo (298 °C), sm exo (510 °C).

^{17}O Precursors. ^{17}O (20% enriched) HO**neo*-Pe (Isotech) was used as received. Crystalline material was used for all analyses.

(a) $[Ti(O^*neo\text{-}Pe)_4]_2$ (1*). Ti(OPr^i)$_4$ was reacted with 4.5 HO**neo*-Pe to yield **1*** under identical conditions used for the synthesis of **1**.[7] Analytical data of **1*** were consistent with that of **1**.

(b) AO*neo-Pe. NaO**neo*-Pe and KO**neo*-Pe were produced by the reaction of the appropriate alkali metal hydride and (excess) HO**neo*-Pe. Analytical data of the enriched species (AO**neo*-Pe) was consistent with the AO*neo*-Pe species.

(c) $[ATi(O^*neo\text{-}Pe)_5]_2$. The synthesis of $[NaTi(O^*neo\text{-}Pe)_5]_2$ (**3***) and $[KTi(O^*neo\text{-}Pe)_5]_2$ (**4***) were isolated using **1*** and the appropriate AO**neo*-Pe under identical conditions reported for **3** and **4**.

X-ray Collection, Structure Determination, and Refinement. Colorless crystals of **2** and **4** with approximate dimensions of 0.20 × 0.40 × 0.43 mm and 0.33 × 0.47 × 0.50 mm, respectively, were mounted individually onto a glass fiber and transferred to a Siemens P4 diffractometer. The determination of Laue symmetry, crystal class, unit cell parameters, and crystal orientation matrix were carried out according to standard procedures.[10] Intensity data were collected at low temperature using a $2\theta/\omega$ scan technique with Mo Kα radiation. The raw data were processed with a local version of CARESS,[11] which employs a modified version of the Lehman−Larsen algorithm to obtain intensities and standard deviations from the measured 96-step peak profiles. Subsequent calculations were carried out using the SHELXTL program.[12]

For **2**, all 4287 data were collected at 158 K and were corrected for Lorentz and polarization effects and placed on an approximately absolute scale. There were no systematic absences nor any diffraction symmetry other than the Fiedel condition. The centrosymmetric triclinic space group $P\bar{1}$ was assigned and later determined to be correct. The structure was solved by direct methods and refined on F^2 by full-matrix least-squares techniques. The analytical scattering factors for neutral atoms were used throughout the analysis.[13] Hydrogen atoms were included using a riding model. The molecule is located about an inversion center. At convergence, $R_{w2} = 0.1373$ and GOF = 1.030 for 309 variables refined against 4026 unique data (as a comparison for refinement on F, $R_1 = 0.506$ for those 3012 data with $F > 4.0\sigma(F)$).

For **4**, all 5942 data were collected at 163 K and were corrected for Lorentz and polarization effects and placed on an approximately absolute scale. The diffraction symmetry was 2/*m* with systematic absences for 0*k*0 for $k = 2n + 1$ and *h*0*l* for $h + l = 2n + 1$. The centrosymmetric monoclinic space group $P2_1/n$ is therefore uniquely defined. The structure was solved by direct methods and refined on F^2 by full-matrix least-squares techniques. The analytical scattering factors for neutral atoms were used throughout the analysis.[13] Hydrogen atoms were included using a riding model. The molecule is located about an inversion center. Carbon atoms C(21), C(24), and C(25) are disordered. These atoms were included with two components each with site-occupancy factors of 0.60 and 0.40 for the major and minor components.

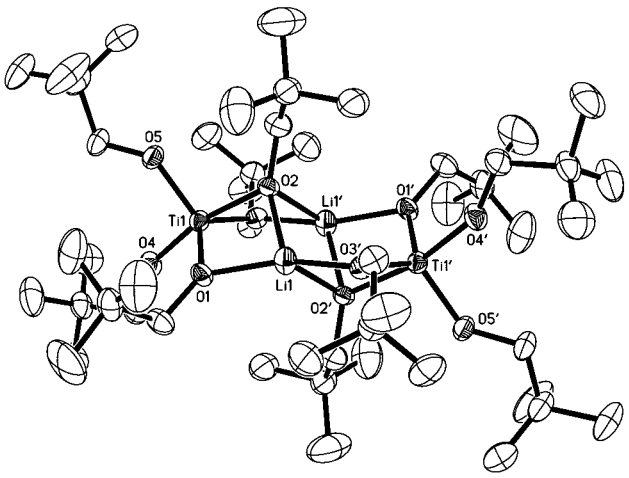

Figure 2. Thermal ellipsoid plot of [LiTi(O*neo*-Pe)$_5$]$_2$, **2**. Thermal ellipsoids are drawn at the 30% level.

Hydrogen atoms associated with C(23) were not included in the refinement. At convergence, $R_{w2} = 0.3137$ and GOF = 1.021 for 176 variables refined against 5707 unique data (as a comparison for refinement on F, $R_1 = 0.1016$ for those 3487 data with $F > 4.0\sigma(F)$).

Results and Discussion

The syntheses, solid-state structures, and solution properties of the alkali metal derivatives of **1** are described in detail. Due to the well-characterized species of $[ATi(OPr^i)_5]_n$ (see Figure 1A−C), the O*neo*-Pe derivatives were also crystallographically characterized. These compounds were generated to study the influence that the O*neo*-Pe ligand had on both the solution and solid-state behavior of the ATi(OR)$_5$ compounds.

Synthesis. Alkali metal modified **1** compounds, **2**−**4**, were isolated from the reaction mixture of preformed and purified AO*neo*-Pe and **1** (eq 4). Each component was individually dissolved in toluene and, upon dissolution, combined. If an

$$[Ti(O\textit{neo}\text{-}Pe)_4]_2 + 2AO\textit{neo}\text{-}Pe \rightarrow [ATi(O\textit{neo}\text{-}Pe)_5]_2 \quad (4)$$
$$A = Li, Na, K$$

insufficient amount of solvent were used, a precipitate formed which could not be dissolved by heating or through the addition of additional HO*neo*-Pe. However, a clear solution could be obtained through dilution with additional toluene followed by a slight warming of the reaction mixture. The larger alkali metal cations required less solvent to obtain a clear solution which is consistent with a reduction in solution oligomerization as was found for **3** and **4** (vide infra). Crystals suitable for single-crystal X-ray analyses were isolated by allowing the warmed reaction mixtures to cool to glovebox temperatures. These yields were never optimized since the analytical data of the bulk powders (isolated by drying the reaction mixture by rotary evaporation) were consistent with the crystalline materials. Acceptable elemental analyses of the bulk materials were not be obtained, which is most likely due to the volatility of the alkali metal[14] under the thermal conditions (950 °C) used in the analyses.

The thermal ellipsoid plots of **2** and **4** are shown in Figures 2 and 3, respectively. These compounds were isolated in a standard $[ATi(O\textit{neo}\text{-}Pe)_5]_2$ arrangement. Interestingly, **2** was also formed in low yield from the reaction mixture of **1** with LiCMe$_3$ in toluene. Since both the larger and smaller congeners

(10) *XSCANS Software Users Guide*, Version 2.1; Siemens Industrial Automation, Inc.; Madison, WI, 1994.
(11) Broach, R. W. *CARESS*; Argonne National Laboratory, Argonne, IL, 1978.
(12) Sheldrick, G. M. *SHELXTL*; Siemens Analytical X-ray Instruments, Inc.: Madison WI, 1994.
(13) *International Tables for X-ray Crystallography*; Kluwer Academic Publishers: Dordrecht, The Netherlands, 1992; Vol. C.
(14) Voigt, J. A.; Boyle, T. J.; Doughty, D. H.; Hernandez, B. A.; Johnson, B. J.; Levy, S. C.; Tafoya, C. J.; Rosay, M. *Mater. Res. Soc. Symp. Proc.* **1995**, *393*, 101.

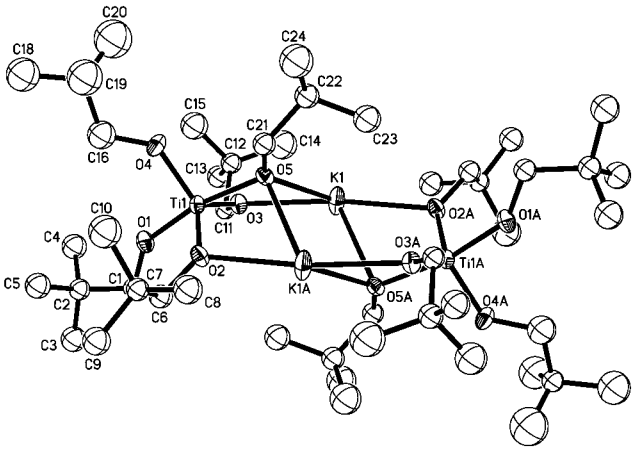

Figure 3. Thermal ellipsoid plot of $[KTi(O\textit{neo}\text{-}Pe)_5]_2$, **3**. Thermal ellipsoids are drawn at the 50% level.

Table 1. Crystallographic Collection Data for $[LiTi(OCH_2CMe_3)_5]_2$, **2**, and $[KTi(OCH_2CMe_3)_5]_2$, **4**

	2	**4**
chem formula	$C_{50}H_{110}Li_2O_{10}Ti_2$	$C_{50}H_{110}K_2O_{10}Ti_2$
fw	981.06	1045.38
temp (K)	158	163
space group, system	$P\bar{1}$, triclinic	$P2_1/n$, monoclinic
a (Å)	10.656 (3)	15.060 (4)
b (Å)	12.202 (5)	12.264 (3)
c (Å)	13.266 (3)	18.150 (5)
α (deg)	75.39 (2)	
β (deg)	73.31 (2)	104.90 (1)
γ (deg)	71.65 (2)	
V (Å^3)	1543.3 (8)	3239.5 (14)
Z	1	2
λ (Mo Kα radiation) (Å)	0.710 73	0.710 73
D_{calcd} (Mg/m^3)	1.056	1.072
μ(Mo Kα) (mm^{-1})	0.304	0.419
R_1[a] % [$I > 2\sigma(I)$]	5.06	10.16
R_1[a] % (all data)	7.64	15.74
R_{w2}[b] % [$I > 2\sigma(I)$]	11.99[c,e]	25.90[d,e]
R_{w2}[b] % (all data)	13.73[c,e]	31.37[d,e]

[a] $R_1 = \sum||F_o| - |F_c||/\sum|F_o|$. [b] $R_{w2} = \{\sum[w(F_o^2 - F_c^2)^2]/\sum[w(F_o^2)^2]\}^{1/2}$. [c] $w = 1/[\sigma^2(F_o^2) + (0.0631P)^2 + 1.7823P]$. [d] $w = 1/[\sigma^2(F_o^2) + (0.1491P)^2 + 16.0352P]$. [e] $P = (F_o^2 + 2F_c^2)/3$.

favored the tetranuclear dimeric formation, the structure of the Na derivative was assumed to possess an analogous structure. Further investigations to confirm the structure of **3** and determine the solution behavior of **2**−**4** were performed.

Solid State

Crystal Structure. Single-crystal X-ray diffraction studies were undertaken to discern the solid-state structures of **2** and **4**, which are shown in Figures 2 and 3, respectively. Table 1 lists the collection parameters for **2** and **4**. Table 2 is a tabulation of the metrical data for **2** and **4**. The solid-state structures of $[LiTi(OPr^i)_5]_2$,[5,15] **2**, and **4** were all characterized in a standard M_4O_{16}-like arrangement,[5,15−18] wherein the titanium metal center adopts a distorted trigonal-bipyramidal (tbp) geometry and each alkali metal center is in a tetrahedral arrangement using two μ-OR and two μ_3-OR ligands. In contrast the solid-state structure of the heavier alkali metal derivatives of $[ATi(OPr^i)_5]_\infty$, where A = Na and K, are four- and five-coordinated, respectively.

The Ti−O bond distances of **2** and **4** are consistent with literature reports and, as is typically observed for titanium alkoxide complexes,[5,15−18] aggrandize with increased bonding: (i) for **2**, O*neo*-Pe_{term} (av 1.82 Å) < μ-O*neo*-Pe (av 1.92 Å) < μ_3-O*neo*-Pe (2.029 Å), and (ii) for **4**, O*neo*-Pe_{term} (av 1.83 Å) < μ-O*neo*-Pe (av 1.89 Å) < μ_3-O*neo*-Pe (1.999 Å). The terminal and Ti−(μ-OR) distances of **2** and **4** are in agreement with the $[ATi(OPr^i)_5]_n$ derivatives; however, the Ti−(μ_3-O) distances of **2** and **4** are significantly longer than the OPr^i derivatives. The A−O distances also lengthen with increased bonding: (i) for **2**, μ-O*neo*-Pe (av 1.95 Å) < μ_3-O*neo*-Pe (av 2.01), and (ii) for **4**, μ-O*neo*-Pe (av 2.59 Å) < μ_3-O*neo*-Pe (av 2.68). These distances also correlate with the OPr^i derivatives. The one exception is the K−(μ_3-O*neo*-Pe) distances which are significantly longer for the OPr^i derivative (2.784(1)Å) due to the structural differences noted for these compounds (Figures 1C and 3).

There is little difference in the angles around the tbp Ti metal center of **2**, **4**, and $[LiTi(OPr^i)_5]_2$. The axial alkoxides of the tbp titanium metal centers act as the bridging ligands to force a distorted geometry around the alkali metal center. The reduction of the idealized 180° angle for the (OR)−Ti(1)−(μ_3-OR) angle of **2** and **4** to ∼167° results in the expansion of the idealized 120° angle for the (μ-OR)−Ti(1)−(μ-OR) angle to ∼125°. This strain, due to the steric demands of the alkoxide, results in a severe distortion of the four-coordinated alkali metal's geometry. The (μ-OR)−A−(μ-OR) angles for **2** and $[LiTi(OPr^i)_5]_2$ are similar to the very distorted tetrahedron arrangements that were reported for $[LiTi(OPr^i)_5]_2$[15] and $[LiSn(OBu^t)_3]_2$.[19,20] However, for **4**, the same angle O(3)−K(1)−O(2a) approaches linearity (172.7°); thus, K is forced into an irregular C_{2v} arrangement, adopting a pseudo tbp geometry.[21] Any angular comparisons between **4** and $[KTi(OPr^i)_5]_n$ are difficult due to the changes in K coordination.

Previously, a correlation between the alkali/titanium cation ratio (A/M) was presented as a means to determine oligomerization in the solid state.[5] This was based on a limited data set; however, with the isolation of **2** and **4** as molecular compounds this proposal must be redefined. The Ti−O bond distances of the OPr^i and O*neo*-Pe are statistically equivalent which indicates that the electronic contribution of the two ligands to the final structure are nearly identical. Therefore, the shape and steric bulk of the pendant hydrocarbon chain of the alkoxide ligand plays a pivotal role in determining the final structure adopted in the solid state. Structural evidence suggests that early transition metal O*neo*-Pe ligated complexes consistently form either identical[8] or smaller[9,22] nuclearity complexes in comparison to the structures of OPr^i ligated species. Hence, the O*neo*-Pe ligand may be considered to possess slightly greater steric bulk in comparison to the OPr^i ligand. This slight increase in steric bulk may explain the characterization of molecular species for the O*neo*-Pe ligated complexes. Molecular modeling experiments, to determine energetically favored states, are being considered as a means of evaluating molecular versus polymer formation.

Solid-State NMR. A series of multinuclear experiments involving ^{17}O, ^{13}C, and ^{x}A were undertaken to aid in the solid-

(15) Hampden-Smith, M. J.; Williams, D. S.; Rheingold, A. L. *Inorg. Chem.* **1990**, *29*, 4076.
(16) Wright, D. A.; Williams, D. A. *Acta Crystallogr., Sect. B* **1968**, *24*, 1107.
(17) Ibers, J. A. *Nature (London)* **1963**, *197*, 686.
(18) Boyle, T. J.; Schwartz, R. W.; Doedens, R. J.; Ziller, J. W. *Inorg. Chem.* **1995**, *34*, 1110.
(19) Veith, M.; Rosler, R. *Z. Naturforsch* **1986**, *41B*, 1071.
(20) Veith, M.; Rosler, R. *Angew. Chem., Int. Ed. Engl.* **1982**, *21*, 858.
(21) Cotton, F. A.; Wilkinson, G. *Advanced Inorganic Chemistry* 5th ed.; John Wiley & Sons: New York, 1988.
(22) Boyle, T. J.; Tafoya, C. J.; Scott, B. L. *Abstr. Pap.—Am. Chem. Soc.* **1996**, *211* (1), 62-INOR.

Table 2. Comparison of the Interatomic Distances (Å) and Angles (deg) for **2** and **4**

	2		**4**	
distances (Å)				
Ti···Ti′				
A···Ti[a]	Li(1)−Ti(1)	2.951 (6)	K(1)−Ti(1)	3.688 (2)
	Li(1)−Ti(1a)	2.922 (6)	K(1a)−Ti(1)	3.663 (2)
	Li(1a)−Ti(1)	2.922 (6)		
A···A′	Li(1)−Li(1a)	2.661	K(1)···K(1a)	3.664
Ti−(OR)[b]	Ti(1)−O(5)	1.813(2)	Ti(1)−O(1)	1.835 (4)
	Ti(1)−O(4)	1.819 (2)	Ti(1)−O(4)	1.817 (5)
Ti−(μ-OR)	Ti(1)−O(3)	1.919 (2)	Ti(1)−O(2)	1.897 (5)
	Ti(1)−O(1)	1.917 (2)	Ti(1)−O(3)	1.890 (4)
Ti−(μ_3-OR)	Ti(1)−O(2)	2.029 (2)	Ti(1)−O(5)	1.999 (4)
A−(μ_3-OR)	Li(1)−O(2)	1.972 (6)	K(1)−O(5)	2.673 (5)
	Li(1)−O(2a)	2.040 (6)	K(1)−O(5a)	2.696 (5)
A−(μ-OR)	Li(1)−O(1)	1.948 (6)	K(1)−O(2a)	2.587 (5)
	Li(1)−O(3a)	1.952 (6)	K(1)−O(3)	2.587 (5)
angles (deg)				
(OR)−Ti−(OR)	O(4)−Ti(1)−O(5)	97.60 (11)	O(1)−Ti(1)−O(4)	96.3 (2)
(OR)−Ti−(μ-OR)	O(4)−Ti(1)−O(3)	94.38 (11)	O(1)−Ti(1)−O(2)	91.9 (2)
	O(4)−Ti(1)−O(1)	95.13 (11)	O(4)−Ti(1)−O(2)	114.6 (2)
	O(5)−Ti(1)−O(1)	117.43 (11)	O(1)−Ti(1)−O(3)	91.9 (2)
	O(5)−Ti(1)−O(3)	115.93 (11)	O(1)−Ti(1)−O(3)	91.9 (2)
(μ-OR)−Ti−(μ-OR)	O(1)−Ti(1)−O(3)	123.74 (10)	O(2)−Ti(1)−O(3)	127.5 (2)
(OR)−Ti−(μ_3-OR)	O(4)−Ti(1)−O(2)	167.12 (10)	O(1)−Ti(1)−O(5)	168.5 (2)
	O(5)−Ti(1)−O(2)	95.27 (10)	O(4)−Ti(1)−O(5)	95.2 (2)
(μ-OR)−Ti−(μ_3-OR)	O(1)−Ti(1)−O(2)	78.80 (10)	O(2)−Ti(1)−O(5)	83.1 (2)
	O(3)−Ti(1)−O(2)	79.97 (10)	O(3)−Ti(1)−O(5)	83.1 (2)
(μ-OR)-A-(μ-OR)	O(1)−Li(1)−O(3a)	157.8 (3)	O(3)−K(1)−O(2a)	172.7 (2)
(μ-OR)−A−(μ_3-OR)	O(1)−Li(1)−O(2)	79.5 (2)	O(3)−K(1)−O(5)	58.76 (13)
	O(1)−Li(1)−O(2a)	111.5 (3)	O(2a)−K(1)−O(5)	119.2 (2)
			O(2a)−K(1)−O(5a)	58.57 (13)
(μ_3-OR)−A−(μ_3-OR)	O(2)−Li(1)−O(2a)	96.9 (3)	O(5)−K(1)−O(5a)	93.92 (14)
A−(μ_3-OR)−A′	Li(1)−O(2)−Li(1a)	83.1 (3)	K(1)−O(5)−K(1a)	86.08 (14)
A−(μ_3-OR)−Ti	Li(1)−O(2)−Ti(1)	95.0 (2)	K(1)−O(5)−Ti(1)	103.3 (2)
	Li(1a)−O(2)−Ti(1)	91.8 (2)	K(1a)−O(5)−Ti(1)	101.5 (2)
A−(μ-OR)−Ti	Li(1)−O(1)−Ti(1)	99.5 (2)	K(1)−O(3)−Ti(1)	109.9 (2)
	Li(1a)−O(3)−Ti(1)	98.0 (2)	K(1a)−O(2)−Ti(1)	108.6 (2)

[a] A = Li, K. [b] OR = OCH_2CMe_3.

Table 3. MAS Solid-State and Solution-State NMR Data for the Parent AO*neo*-Pe and **2**−**4**

	LiO*neo*-Pe	**2**	NaO*neo*-Pe	**3**	KO*neo*-Pe	**4**
			Solid State[a]			
$^{13}C\{^1H\}$						
OCH_2CMe_3	76.8	88.4, 83.6, 82.7, 79.2	75.3, 72.6	87.8, 82.9, 80.7	80.4, 75.4	86.9, 83.1, 81.5, 79.2
OCH_2CMe_3	34.2	34.5, 33.8	39.3, 34.8, 33.9, 33.3, 32.8	34.1	40.0, 36.9	34.4, 34.0, 33.6
OCH_2CMe_3	27.3	28.0, 27.1, 26.7	28.3, 27.8, 27.2	28.6, 27.6, 26.5	28.7	28.5, 27.5, 27.0
[x]A	(^{6}Li) 0.56 (^{7}Li) −0.04.	(^{6}Li) 0.44 (^{7}Li) 0.06	(^{23}Na) 10.0, 7.24, −8.47	(^{23}Na) −14.69	(^{39}K) N.O.[e]	(^{39}K) N.O.
			Solution State[b]			
[x]A	(^{7}Li) 1.36	(^{7}Li) 1.57, 1.36, 1.00	(^{23}Na, 75 °C) 6.24	(^{23}Na, 75 °C) 3.14	(^{39}K) N.O.	(^{39}K) N.O.

[a] Referenced against the secondary solid-state standard: the carbonyl resonance of glycine (δ = 176.0 ppm versus neat TMS δ = 0.00 ppm) for ^{13}C; 1 M LiCl (δ = 0.0 ppm) for ^{6,7}Li; 1 M NaCl (δ = 0.0 ppm) for ^{23}Na. [b] Chemical shifts are in parts per million at room temperature in toluene-d_8. [e] N.O. = not obtained.

state characterization of the O*neo*-Pe derivatives. Table 3 lists the resonances observed for **2**−**4** and the corresponding starting AOR.

The ^{17}O MAS NMR spectra obtained for the ^{17}O labeled derivatives (LiO**neo*-Pe, KO**neo*-Pe, **3***, and **4***) possessed disproportionally broad peaks with a low signal-to-noise ratio. There were significant variations between the ^{17}O MAS spectra of the AO**neo*-Pe and $[ATi(O*neo\text{-}Pe)_5]_2$; however, conclusive structural information could not be discerned. For **3*** and **4***, resonances consistent with a variety of oxygen environments (μ_3-O*neo*-Pe, μ-O*neo*-Pe, and O*neo*-Pe_{term}) were observed.

The ^{13}C CP-MAS spectrum of **2** had the following resonances: methyl (δ 28.8, 27.1, 26.4), quaternary carbon (δ 34.4, 33.8), and methylene (88.4, 83.6, 82.7, 79.2 (minor)). Since the structure of **2** was isolated in a centrosymmetric space group with an inversion center, there should be three types of O*neo*-Pe ligands (OR_{term}, μ-OR, μ_3−OR) present in a 2:2:1 ratio. The lack of a sufficient number of observed quaternary carbons may be explained by coincidental overlap. The minor methylene peak may reflect disorder in the crystal lattice. A similar spectrum was recorded for **4**, wherein the ^{13}C CP-MAS NMR spectrum also revealed three sets of O*neo*-Pe resonances with very small shoulders present for each resonance. For **4** the additional shoulders may again represent disorder in the solid-state structure or a manifestation of the two inequivalent molecules located in the unit cell. The ^{13}C CP-MAS spectrum of the AO*neo*-Pe derivatives were significantly varied from either **2** or **4**.

Since **3** was not structurally characterized, inferences about the solid-state structure must be made from the spectra reported for **2** and **4**. Again the spectrum of the parent NaO*neo*-Pe was significantly varied from that of **3**. The ^{13}C CP-MAS NMR

spectrum of **3** has three sets of methyl and methylene resonances present, but only one quaternary carbon resonance was observed. A minor fourth methylene peak was observed in the ^{13}C NMR spectrum of **3***. Overlap of the quaternary carbon resonances is expected on the basis of the observed spectra of **2** and **4**, and the minor peaks observed for **3*** were also observed for **2** and **4**. Since the ^{13}C spectra of **3** are consistent with **2** and **4**, these compounds must also possess similar solid-state moieties.

To further investigate the structural aspects of the solid-state structure of **2**−**4**, alkali metal NMR studies were undertaken. If **2**−**4** all adopt the $[ATi(O\textit{neo}\text{-}Pe)_5]_2$ structure, only one type of alkali metal should be observed in the solid state.

Both ^6Li (spin $I = 1$) and ^7Li (spin $I = {}^3/_2$) may possess a quadrupolar interaction in the solid state, and even under fast MAS NMR conditions a second-order isotropic quadrupolar induced shift may be present. Therefore, the experimentally observed NMR shift of the Li nucleus is the sum of the second-order quadrupolar shift and the true isotropic chemical shift. Unfortunately, the ^7Li MAS shift includes the second-order quadrupolar induced shift. In comparison, the quadrupolar moment of the ^6Li nucleus is relatively small (∼50 times smaller than in ^7Li) and any quadrupolar induced shift is negligible; hence, the ^6Li shift is equal to the true isotropic chemical shift and should be used to discuss changes in structure. Comparison of the shifts observed in the ^6Li and ^7Li MAS experiments reflects the influence of this quadrupolar interaction.[23] The ^6Li and ^7Li MAS NMR spectra of **2** have one resonance each at δ −0.04 and +0.07 ppm, respectively, and were significantly varied from that of LiO*neo*-Pe (^6Li, δ +0.56; ^7Li, δ −0.04). The difference between the ^6Li and ^7Li shifts in these two compounds are $\Delta\nu = 0.11$ ppm for **2** and $\Delta\nu = 0.60$ ppm for LiO*neo*-Pe which indicates that the Li in LiO*neo*-Pe possesses a larger second-order quadrupolar interaction in comparison to that of **2**. This suggests that the Li of **2** exists in a higher symmetry environment than that of LiO*neo*-Pe. An increase in local symmetry over the LiO*neo*-Pe precursor would be consistent with the general aspects of the crystal structure of **2**.

The ^{23}Na NMR spectrum of **3** has only one broad peak centered around −14 ppm, whereas the ^{23}Na NMR spectrum of the O*neo*-Pe ligand consisted of a singlet at +10.0 ppm (major) and two smaller peaks at +7.24 and −8.47 ppm (very broad). The single ^{23}Na signal for the bulk sample of **3** would be consistent with the proposed $[NaTi(O\textit{neo}\text{-}Pe)_5]_2$ structure. Unfortunately, ^{39}K MAS NMR spectra could not be obtained due to the low sensitivity of this nucleus.

While a crystal structure of **3** is required for the unequivocal characterization of this complex in the solid state, some general inferences concerning the solid-state structure of **3** can be made on the basis the data collected for this congener series. The single alkali metal signal observed for **2** and **3** and the similarities of the ^{13}C spectra of **2**−**4** indicate that **3** has a structure similar to that of **2** and **4.** Therefore, we tentatively assign the solid-state structure of **3** as $[NaTi(O\textit{neo}\text{-}Pe)_5]_2$.

FT-IR. The FT-IR spectra of **2**−**4** were nearly superimposable. A simplification in the aliphatic stretches (2500−3000 cm^{-1}) and three stretches associated with the various Ti−O stretches (600−700 cm^{-1}) were noted for **2**−**4** in comparison to the parent AOR spectra.

TGA/DTA. The thermal decomposition of these compounds monitored by TGA/DTA under an oxygen atmosphere appeared to be very similar. For each compound there is one major weight loss around 200 °C, observed in the TGA, accompanied by a large exotherm in the DTA. Typically, two small weight losses follow this large thermal event accompanied by a small exotherm. The second exotherm is representative of the crystallization of the amorphous material. Since both **2** and **3** have exotherms ∼2 times larger than that of **1**, it is assumed that a number of decomposition steps occur for **2** and **3** over this temperature range and may explain why **1** has a slightly more complicated DTA spectrum. As the size of the alkali metal increases, the crystallization temperature increases as well [Li (330 °C) < Na (381 °C) < K (518 °C)].

Solution State

Molecular Weight. Isopiestic molecular weight studies (Signer method[24]) were not possible for **2** or **3** due to their low solubility in toluene. Compound **4** was soluble enough in toluene to allow for a molecular complexity (MC) to be determined as ∼1/2 (av MW 517 ± 25) the solid-state structure at a concentration of 0.1 M. This is consistent with a dimeric species, symmetrically disrupting to form the monomer species in solution. In contrast, the OPr^i derivatives were found to be dinuclear in solution for each alkali metal derivative;[5,15] however, the OPr^i derivative MC determinations were performed using cryoscopic molecular weight determinations at ∼0.02 M due to their low solubility.[15]

Solution-State NMR. Since solution MC could not be confirmed for all of these samples, solution-state NMR studies were undertaken to elucidate the solution behavior of these compounds. Crystalline samples of **2**−**4** were dissolved in toluene-d_8 to obtain their ^1H, ^{13}C, and alkali metal nuclei (^xA) solution NMR spectra. The spectral results are transcribed in Table 3. Saturated samples of **2**−**4** were used for each experiment.

A ^1H NMR spectrum of a saturated sample of **2** was collected at room temperature which had two sets of O*neo*-Pe resonances in a 1:1.8 resonance. This is *not* consistent with the solid-state structure since either a 1:2:2 (μ_3-OR:μ_2-OR:OR_{term}), 1:4 (μ_3-OR:μ_2-OR and OR_{term}), or even the unlikely ratio of 2:3 (μ_2-OR:μ_3-OR and OR_{term}) should be observed for the various combinations of terminal and bridging ligands present in the solid-state structure. The $^{13}C\{^1H\}$ NMR spectrum also indicates two sets of O*neo*-Pe ligands are present with the resonances of the quaternary carbons coincidentally overlapping. Dilution of the sample resulted in a change in the ratio of the observed resonances. This suggests that an equilibrium exists which can easily be envisioned as a disruption of the dimer into two monomers (eq 5a). Variable temperature ^1H NMR (VT-NMR)

$$\underset{\text{"dimer"}}{[ATi(O\textit{neo}\text{-}Pe)_5]_2} \leftrightarrows \underset{\text{"monomer"}}{2ATi(O\textit{neo}\text{-}Pe)_5} \quad (5a)$$

$$ATi(O\textit{neo}\text{-}Pe)_5 \leftrightarrows Li(O\textit{neo}\text{-}Pe) + Ti(O\textit{neo}\text{-}Pe)_4 \quad (5b)$$

experiments were undertaken to clarify the solution behavior of **2**. No coalescence/decoalescence of the O*neo*-Pe resonances were observed in the temperature range investigated; instead with a change in temperature the two methylene peaks of the ^1H NMR spectrum change intensity. This is further evidence that a nuclearity exchange or equilibrium (eq 5a) is occurring. At room temperature, the ^7Li NMR reveals only one peak present at 0.81 ppm but it is relatively broad for ^7Li resonances. This was assigned as the tetranuclear dimeric species since the larger oligomer would be favored at lower temperatures.[1]

(23) Boyle, T. J.; Ingersoll, D.; Alam, T. M.; Rodriguez, M. A.; Vanheusden, K.; Doughty, D. H. *Chem. Mater.* **1998**, *10*, 2270.

(24) (a) Clark, E. P. *Analytical Edition* **1941**, 820. (b) Signer, R. *Ann.* **1930**, *478*, 246.

Elevated temperature (~70 °C) ^{7}Li spectra were also obtained, and, surprisingly, three ^{7}Li resonances were recorded. One of these resonances was consistent with LiO*neo*-Pe. A 2D ^{7}Li NMR experiment at this temperature revealed rapid exchange between two of the three inequivalent lithium nuclei at this temperature (one of these was the LiO*neo*-Pe resonance). Therefore, it is reasonable to assume that, at high temperatures, an additional equilibrium is introduced that represents the breakdown of the monomer into its constituent components (eq 5b).

One complete set of ^{1}H and ^{13}C NMR O*neo*-Pe resonances was recorded for **3** in toluene. Again, either rapid exchange of the various ligands or disruption of the solid-state structures would explain the observed spectrum. The ^{23}Na NMR spectrum had only one very broad peak which did not shed light on the nuclearity of the solution complex. ^{1}H VT-NMR (−30 to +65 °C) revealed an upfield shift of the methylene peak as the temperature was increased; however, there is no change in the number of peaks (*note*: the full width at half-maximum sharpens significantly at higher temperatures). Sufficiently low temperatures could not be reached to observe decoalescence. To further elucidate the solution behavior of **3**, **3*** (^{17}O labeled) was synthesized to investigate the oxygen environments of this molecule. All of the analytical data were consistent between **3** and **3*** except for the solid-state ^{13}C NMR data, wherein a more pronounced shoulder was visible in the methylene resonances of the spectrum of **3***. For retention of the solid-state structure in solution, one would expect to observe three types of oxygen resonances (terminal, μ, and μ_3).[25] For **3*** in toluene-d_8, there was only one resonance (δ 248), the shift of which is consistent with terminal O*neo*-Pe ligands.[6] One explanation of the observed singlet would be the formation of a tight ion pair such as "Na^{+-}Ti(O*neo*-Pe)$_5$" through the disruption of the solid-state dimer. This behavior was also observed for the larger alkali metal derivatives of the OPr^{i} ligated species.[5]

There are multiple resonances noted for the ^{1}H NMR spectrum of **4**. The ^{13}C NMR spectrum reveals two types of O*neo*-Pe ligands (spectrum was collected at high temperature due to low solubility at room temperature). VT NMR reveals a great deal of dynamic behavior associated with rapid ligand exchange but not an equilibrium. These spectra are consistent with the monomer being present in toluene. Compound **4*** (^{17}O enriched with analytical data was consistent with **4**) had one broad peak in the ^{17}O CP-MAS NMR ranging from δ 243 to 232 and is consistent with terminal O*neo*-Pe ligands. These data, coupled with the MW determination (vide infra), indicate that the monomer is the preferred nuclearity for **4** in toluene, again acting as a tight ion pair.

Conclusion

Reactivity studies of [Ti(μ-O*neo*-Pe)(O*neo*-Pe)$_3$]$_2$ with AO*neo*-Pe (A = Li, **2**; Na, **3**, K, **4**) result in the isolation of the [ATi(O*neo*-Pe)$_5$]$_2$ complexes in the solid state, independent of the alkali metal used. This is in contrast to the OPr^{i} derivative, wherein the Na and K adducts were found to be polymeric in the solid state. It is ventured that the steric bulk of the O*neo*-Pe ligand is sufficiently greater in comparison to the OPr^{i} ligand to favor the formation of molecular species for the Na and K derivatives. Solution NMR of **2** indicates that at room temperature the solid-state structure is disrupted, resulting in a multinuclear equilibrium which is further complicated at higher temperatures by disruption of the monomer into its constituent parts. For **3** and **4**, the NMR data indicate that dinuclear monomers are the preferred arrangement in solution and probably exist as tight ion pairs.

Acknowledgment. For support of this research, the authors would like to thank the United States Department of Energy under Contract DE-AC04-94AL85000. Sandia is a multiprogram laboratory operated by Sandia Corp., a Lockheed Martin Company, for the United States Department of Energy.

Supporting Information Available: X-ray crystallographic files, in CIF format, for the structure of [ATi(O*neo*-Pe)$_5$]$_2$, [A = Li (**2**) and K(**4**)] are available free of charge via the Internet at http://pubs.acs.org.

IC981143D

(25) Day, V. W.; Eberspacher, T. A.; Klemperer, W. G.; Park, C. W.; Rosenberg, F. S. *Oxygen 17 NMR Study of Titania*; John Wiley & Sons: New York, 1992; pp 257−265.